5-Aza-7-deazaguanine DNA: Recognition and Strand Orientation of Oligonucleotides Incorporating Anomeric Imidazo[1,2-*a*]-1,3,5-triazine Nucleosides

by **Frank Seela***, **Stefan Amberg**, **Alexander Melenewski**, and **Helmut Rosemeyer**

Laboratorium für Organische und Bioorganische Chemie, Institut für Chemie, Fachbereich Biologie/Chemie, Universität Osnabrück, Barbarastr. 7, D-49069 Osnabrück

The base-pairing properties of oligonucleotides containing the anomeric 5-aza-7-deazaguanine 2′-deoxyribonucleosides **1** and **5** are described. The oligonucleotides were prepared by solid-phase synthesis, employing phosphoramidite or phosphonate chemistry. Stable 'purine' · purine duplexes with antiparallel (aps) chain orientation are formed, when the α-D-anomer **5** alternates with the β-D-anomeric 2′-deoxyguanosine (**2**) within the same oligonucleotide chain. Parallel (ps) oligonucleotide duplexes are observed, when the β-D anomer **1** alternates with **2**. A renewed reversal of the chain orientation (ps → aps) occurs when compound **1** pairs with 2′-deoxyisoguanosine (**6**). In all cases, it is unnecessary to change the orientation within a single strand when α-D units alternate with their β-D counterparts. Heterochiral base pairs of **5** (α-D) with 2′-deoxyisoguanosine (β-D) are well accommodated in duplexes with random base composition and parallel chain orientation. Base pairs of **5** (α-D) with 2′-deoxyguanosine (β-D) destabilize duplexes with antiparallel chains.

Introduction. – The 5-aza-7-deazapurine (= imidazo[1,2-*a*]-1,3,5-triazine) nucleosides [1] display a similar shape as the parent purine compounds from which they can be formally constructed by transposition of N(7) to the fusion-site position 5. This leads to a 7-deazapurine structure (purine numbering is used throughout the *General Part*), exhibiting a very stable *N*-glycosylic bond. Despite the fact that 5-aza-7-deaza-2′-deoxyguanosine (**1**) [2] is related to 2′-deoxyguanosine (**2**) as well as 7-deaza-2′-deoxyguanosine (**3**) [3], the absence of the proton at N(1) results in a similar *Watson-Crick* recognition site as that of the pyrimidine nucleoside 2′-deoxy-5-methylisocytidine (**4**). Protonation of **1** at N(1) restores the donor-acceptor pattern of a guanine moiety.

So far, only very few 5-aza-7-deazapurines have been incorporated into oligonucleotides. The base-pairing properties of 5-aza-7-deaza-2′-deoxyisoguanosine of DNA · RNA hybrids have been investigated [4][5]. Our laboratory reported on the duplex stability of oligonucleotides containing the β-D-anomeric 2′-deoxyribonucleoside **1** of 5-aza-7-deazaguanine and verified the existence of a 'purine' · purine base pair between 5-aza-7-deazaguanine and guanine, forming a duplex with parallel chain orientation [6].

We now describe oligonucleotides containing 5-aza-7-deaza-2′-deoxyguanosine (**1**) as well as its α-D-anomer **5**, in particular their incorporation into oligodeoxyribonucleotides in place of 2′-deoxycytidine or 2′-deoxy-5-methylisocytidine (**4**). The various base-pairing possibilities of **1** and **5** with 2′-deoxyguanosine (**2**), 7-deaza-2′-deoxyguanosine (**3**), and 2′-deoxyisoguanosine (**6**) within DNA · DNA duplexes are also evaluated [7]. With regard to this, it will be shown that α-D- and β-D-'purine'

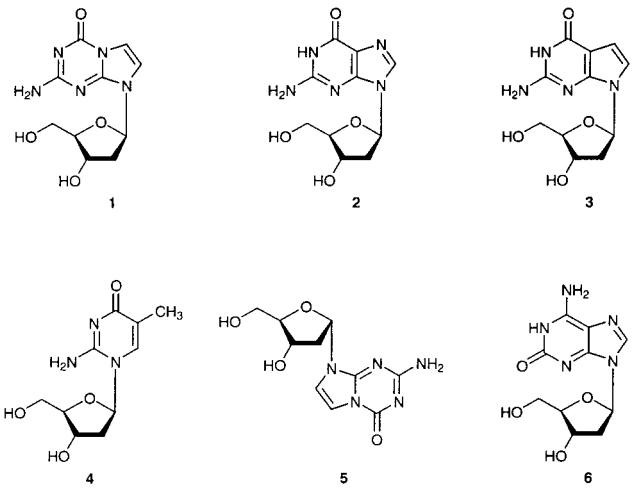

nucleosides in homo- and heterochiral 'purine'·purine base pairs lead to duplex structures with parallel (ps) or antiparallel (aps) chain orientation. The thermal stability of the various duplex structures will be related to their heteromorphous structure.

Results and Discussion. – 1. *Monomers.* The anomers **1** and **5** of 5-aza-7-deaza-2′-deoxyguanosine were prepared as decribed in [2][8]. The β-D-anomer **1** has been already converted into the phosphonates **7** and **8** as well as into the phosphoramidite **9** [6]. These building blocks have been used for the preparation of oligonucleotides [6]; handling and coupling yields during DNA synthesis, however, proved to be not fully satisfactory. Based on this, the α-D-anomer **5** was now first converted into the 3′-phosphonate **10b** [9]. For the synthesis of **10b**, compound **5** was directly transformed into the 5′-(4,4′-dimethoxytrityl) ($(MeO)_2Tr$) derivative **10a** without preceding base protection [10–12]. Subsequent reaction of **10a** with PCl_3/*N*-methylmorpholine/1*H*-1,2,4-triazole gave the desired phosphonate **10b**. As described in the *Exper. Part*, also the use of this building block encountered difficulties and did not give optimal results. Therefore, the work was focussed on the preparation of new phosphoramidite building blocks, *i.e.*, **11** and **18**, for the α-D- as well as for the β-D-anomer **5** and **1**, respectively.

For this purpose, amino-protecting groups, namely the benzoyl as well as various amidine residues, were introduced into both anomers **1** and **5**, and the half-life values of deprotection were measured in conc. aqueous ammonia. Benzoylation of **5** after transient silylation [13] gave the dibenzoyl derivative **10c** in only moderate 52% yield. Because of the two-fold benzoylation and their stepwise hydrolysis in 25% aqueous ammonia, half-life values were determined by reversed-phase HPLC (*RP-18*). From the change of the ratio of peak areas, the rate constants as well as half-life values (τ) of the pseudo-first-order hydrolyses were calculated. While the first benzoyl group was released with a half-life value of 6 min ($k = 0.0987\ min^{-1}$), the second one was removed with a τ of 37 min which corresponds to a rate constant k of $0.0186\ min^{-1}$.

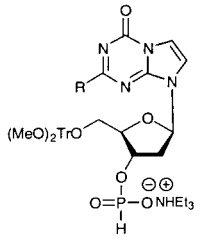

7 R = NH_2
8 R = N=CN(Me)$_2$ (Me)

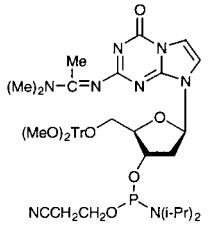

9

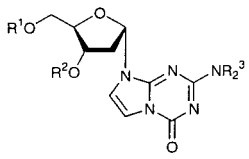

10a R^1 = $(MeO)_2Tr$, R^2 = R^3 = H
b R^1 = $(MeO)_2Tr$, R^2 = $PH(O)O^-$ $\overset{+}{N}HEt_3$, R^3 = H
c R^1 = R^2 = H, R^3 = bz

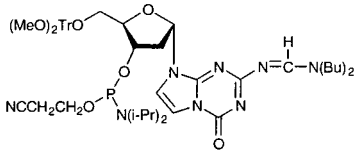

11

Because of the rather low reaction yield upon benzoylation, various N-protecting aminoalkylidene groups were introduced into compound **5**, resulting in an amidine (= imidamide) function (*Scheme 1*) [14][15]. For each reaction, **5** was dissolved in MeOH and treated with an excess of the corresponding dimethyl acetal to give the *N*,*N*-dibutylformimidamide **12a**, the *N*,*N*-diisobutylformimidamide **12c**, the *N*,*N*-dimethylacetimidamide **12b**, and the *N*,*N*-dimethylformimidamide **12d**.

Next, the half-life values (τ) of the various amidine derivatives were determined in 25% aqueous ammonia at 40° and were found to be as follows: **12a**, 126 min; **12b**, 47 min; **12c**, 402 min; **12d**, 3.5 min. As can be seen, the acetimidamide derivative **12b** (τ = 47 min) would be the compound of choice for further reactions. However, it turned out that, upon subsequent dimethoxytritylation, compound **12b** decomposes. As the half-life of the *N*,*N*-dibutylformimidamide **12a** was also suitable, and the introduction of this residue proceeded easily and with high yield (1 h, 40°; 82%), **12a** was chosen for further reactions. Compound **12a** was subsequently protected at the 5′-OH group to give the $(MeO)_2Tr$ derivative **13** in 78% yield. As a by-product, the *N*-formyl derivative **14** was isolated (8% yield), which proved to be very labile under basic conditions (τ (25% aq. NH_3 solution, r.t.) 2 min).

Because the (dibutylamino)methylidene group of the amidine moiety was found to be a suitable protecting group for the α-D-anomer **5**, also the β-D-anomer **1** was now protected in this way yielding compound **15** in 69% (*Scheme 2*). Its half-life (25% aq. NH_3 solution, 40°) amounts to 121 min. Subsequent dimethoxytritylation [16] gave compound **16** (59%), together with the formylated compound **17** (9% yield).

The fully protected α-D- and β-D-anomeric nucleosides **13** and **16**, respectively, were converted into their 3′-phosphoramidites by reaction with 2-cyanoethyl diisopropylphosphoramidochloridite (20 min, r.t.) [17][18]. Both phosphoramidites **11** and **18** were isolated in good yields (83 and 75%, resp.) and were characterized by their ^{1}H- and ^{31}P-NMR spectra.

Scheme 1

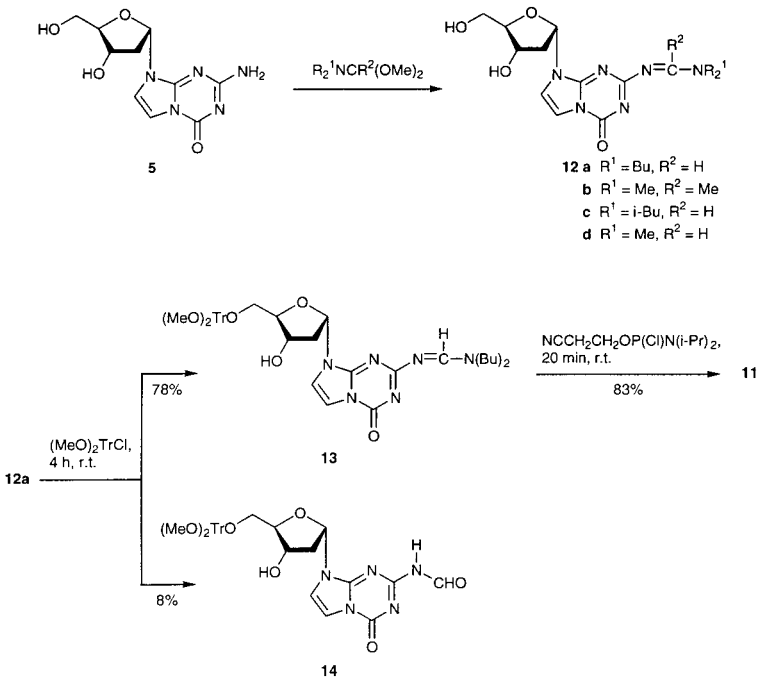

The newly synthesized derivatives were characterized by ^{1}H- and ^{13}C-NMR spectroscopy (*Tables 1* and *2*, and *Exper. Part*). The unequivocal assignment of the ^{13}C-NMR resonances was made on the basis of ^{1}H-coupled ^{13}C-NMR spectra (*Table 2*).

The signals of C(8) and C(4′) of the α-D-anomer **5** are shifted to lower field by 1.4 – 1.8 ppm compared to the β-D-anomer **1**. This effect can be observed for all comparable derivatives of the α-D- and the β-D-series. The introduction of two benzoyl groups (→ **10c**) leads to a high-field shift ($\Delta\delta = 2.5$ ppm) of C(4) of the nucleoside **5**; C(7) and C(8), however, are simultaneously shifted to lower field. All amidine derivatives **12a** – **d** of 5-aza-7-deaza-2′-deoxyguanosine exhibit a characteristic downfield shift of their C(6) resonances (3.9 – 4.1 ppm). Upon 5′-dimethoxytritylation of **12a** and **15**, the usual downfield shifts of the C(5′) signal and a high-field shift of C(4′) were observed.

2. *Oligonucleotides.* 2.1. *Synthesis and Characterization.* Automated solid-phase synthesis of the oligonucleotides **19** – **35** and **38** was performed with the phosphoramidites **11** and **18** as well as standard building blocks [18]. The homomeric oligomers **36** and **37** were prepared with the phosphonates **7** and **10b** (see *Exper. Part*). The syntheses followed the standard protocols [19], and the coupling yields were always higher than 92% for phosphoramidites and *ca.* 90% for phosphonates (see *Table 3*).

Deprotection was performed with conc. aqueous ammonia at 60°. The oligonucleotides were detritylated and purified on purification cartridges[1]) or by reversed-phase HPLC (*RP-18*, see *Exper. Part*). Oligomers with a 3′-terminal-modified

[1]) Oligonucleotide purification cartridges from *Applied Biosystems*, Weiterstadt, Germany.

Scheme 2

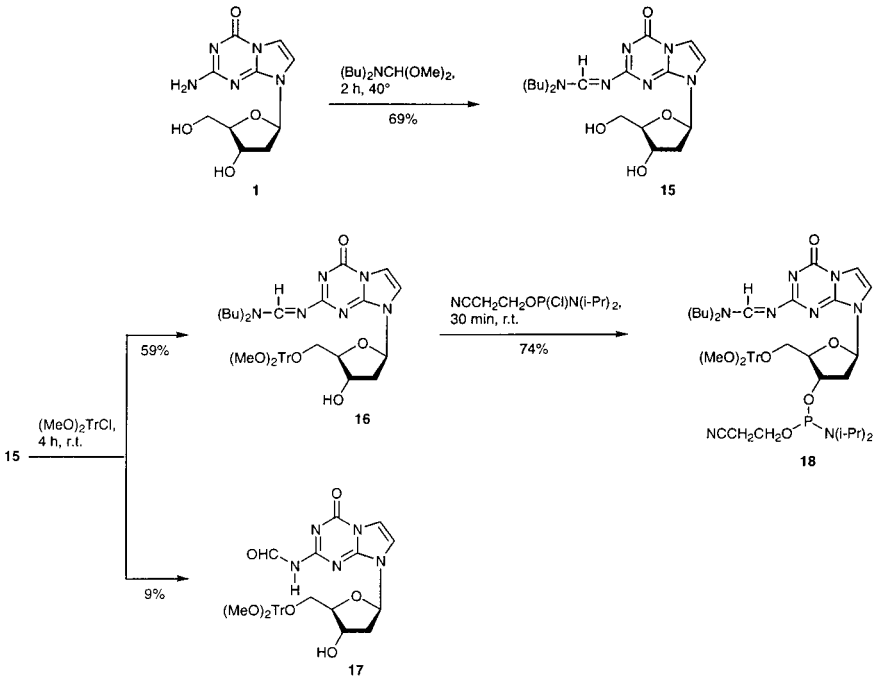

nucleoside residue, *i.e.*, **36**, were synthesized on a universal support with a 3′-terminal ribose moiety[2]). The removal of this residue was carried out upon prolonged treatment with ammonia or in the presence of LiCl (*Exper. Part*). The homogeneity of the compounds was established by HPLC (*RP-18*) as well as by ion-exchange chromatography (*NucleoPac-PA-100* column, 4×50 mm; *Dionex*, P/N 043018, USA). HPLC (*RP-18*) of a mixture of the homomers **36** and **37** showed a slightly higher mobility of the α-D-configurated strand ($\Delta t_R = 1.4$ min). The modified oligonucleotides were characterized by MALDI-TOF mass spectra. The detected masses were in good agreement with the calculated values (*Table 4*).

The composition of the oligonucleotides was determined by tandem hydrolysis with snake-venom phosphodiesterase (SVPDE) and alkaline phosphatase, followed by reversed-phase HPLC (*RP-18*) as described in [20]. Typical reversed-phase HPLC profiles of enzymatic digests of the oligomers **21**, **25**, and **32** are displayed in the *Figure*. It appeared that the SVPDE-catalyzed hydrolysis depends on the structure of the oligonucleotides. Thus, the hydrolyses of the three alternating hexamer duplexes 5′-d(G-C)$_3$-3′ (**39** · **39**),5′-d(G-**1**)$_3$-3′ (**32** · **32**), and 5′-d(G-**5**)$_3$-3′ (**26** · **26**) as well as of the two homomers **36** and **37** were monitored by time-dependent UV measurements at 260 nm, and the half-life values τ were determined (*Table 5*). Within the duplex series, the unmodified oligonucleotide **39** · **39** shows the lowest stability, which is followed by

[2]) *Universal Support 500* (controlled-pore glass), *Glen Research*, Sterling, VA, USA.

Table 1. *^{13}C-NMR Data of 5-Aza-7-deazaguanine Derivatives in (D_6)DMSO at 303 K*

	C(2)[a]) C(2)[b])	C(4)[a]) C(6)[b])	C(6)[a]) C(7)[b])	C(7)[a]) C(8)[b])	C(8a)[a]) C(4)[b])	NCH=N	N–C=N	C=O	C(1′)	C(2′)	C(3′)	C(4′)	C(5′)	MeO	Me–C	Me_2N
5	150.0	165.3	107.9	115.9	150.1	–	–	–	83.5	39.6	70.6	88.9	61.7	–	–	–
1	150.0	165.2	108.3	114.1	150.1	–	–	–	82.6	38.8	70.4	87.5	61.4	–	–	–
10a	150.0	165.3	107.9	115.1	150.0	–	–	–	83.6	38.8	70.9	87.1	63.8	55.0	–	–
b	150.2	165.4	108.1	115.1	150.2	–	–	–	83.9	38.6	73.1	86.3	63.8	55.1	–	–
c	149.5	162.8	108.6	118.4	147.6	–	–	171.9	85.0	[c])	70.3	89.8	61.4	–	–	–
12a	150.2	169.4	107.9	116.5	149.8	159.5	–	–	83.9	[c])	69.8	89.0	60.9	–	–	–
b	150.6	169.2	107.6	116.4	149.6	–	161.5	–	83.9	[c])	70.5	89.0	61.6	–	16.9	[c])
c	150.2	169.4	107.9	116.6	149.7	160.3	–	–	83.8	37.9	70.5	89.0	61.6	–	–	–
d	150.2	169.2	107.8	116.5	149.7	159.7	–	–	83.9	[c])	70.5	89.1	61.7	–	–	34.6
13	150.2	169.5	108.0	116.4	149.8	159.5	–	–	83.9	[c])	70.8	87.0	63.8	55.0	–	–
14	149.6	163.7	108.7	117.0	148.7	–	–	160.9	84.4	[c])	70.8	87.3	63.8	55.0	–	–
15	150.1	169.5	108.4	115.4	149.9	159.5	–	–	83.1	[c])	70.4	87.8	61.4	–	–	–
16	150.1	169.6	108.4	115.3	150.0	159.5	–	–	82.7	[c])	70.1	85.6	63.9	54.9	–	–
17	149.5	163.6	109.0	116.3	148.8	–	–	160.9	83.6	[c])	70.0	85.9	63.8	54.9	–	–

[a]) Systematic numbering. [b]) Purine numbering. [c]) Superimposed by (D_6)DMSO.

Table 2. *^{13}C,^{1}H-Coupling Constants* [Hz] *of Selected 5-Aza-7-deazapurine Derivatives*[a])

C-Atom[b])	Coupling	*J* [Hz]				
		10c	**12a**	**15**	**13**	**14**
C(4)	^{3}J(C(4), H–C(6))	< 1.5	6.8	6.7	6.6	n.d.
N=CH–N or H–C=O	^{1}J(C,H)	–	178.0	178.0	177.9	204.7
C(7)	^{1}J(C(7), H–C(7))	203.6	200.5	200.7	200.3	201.8
	^{2}J(C(7), H–C(6))	11.2	11.5	11.6	11.6	11.8
	^{3}J(C(7), H–C(1′))	4.4	4.9	4.4	4.6	4.5
C(6)	^{1}J(C(6), H–C(6))	208.2	203.9	205.2	205.1	206.4
	^{2}J(C(6), H–C(7))	11.0	11.1	10.6	10.9	11.4
C(8a)	^{3}J(C(8a), H–C(6))[c])	9.0	9.4	9.1	9.4	*ca.* 5
	^{3}J(C(8a), H–C(7))[c])	3.5	3.9	3.4	3.4	*ca.* 5
	^{3}J(C(8a), H–C(1′))[c])	2.0	1.8	2.1	1.8	n.d.
C(1′)	^{1}J(C(1′), H–C(1′))	169.1	169.0	169.5	169.6	172.5
C(4′)	^{1}J(C(4′), H–C(4′))	148.9	149.0	148.0	149.4	148.9
C(3′)	^{1}J(C(3′), H–C(3′))	149.8	150.0	147.8	148.2	150.1
C(5′)	^{1}J(C(5′), H–C(5′))	139.9	140.1	139.8	142.7	142.5

[a]) Measured in (D_6)DMSO at 303 K. [b]) Systematic numbering. [c]) Tentative.

the parallel-stranded all-(β-D)-oligomer 5′-d(G-**1**)$_3$-3′ (**32**·**32**). The antiparallel oligomer **26**·**26** with alternating α-D- and β-D-residues shows a significantly decreased hydrolysis rate. From the two single strands, the α-D-configurated oligomer **36** exhibits a 14-fold longer half-life compared to the β-D-configurated **37**. These results are in agreement with results published earlier on oligonucleotides built-up from nucleotides with α-D-configuration [21].

2.2. *Base Pairing and Duplex Stability of Oligonucleotides.* It has been shown that, in oligodeoxyribonucleotide duplexes, the strands can be inverted from an antiparallel (aps) to a parallel (ps) orientation when in one strand all G_d residues are replaced by 2′-

Table 3. *Oligonucleotide Sequences, Coupling Yields, and Total Yields*

	Oligonucleotide	Coupling yield of modified building blocks **11** or **18**	Yield [A_{260} Units]
19	5′-d(AGT ATT GAC CTA)-3′	–	31
20	5′-d(TAG GTC AAT ACT)-3′	–	56
21	5′-d(AGT ATT GA**5** **5**TA)-3′	100; 100	28
22	5′-d(TAG GT**5** AAT A**5**T)-3′	98; 97	34
23	5′-d(AGT ATT GA**1** **1**TA)-3′	96; 96	18
24	5′-d(TAG GT**1** AAT A**1**T)-3′	100; 97	16
25	5′-d(**5**G**5** G**5**G)-3′	100; 100; 97	11
26	5′-d(G**5**G **5**G**5**)-3′	98; 100; 95	9
27	5′-d(**5**c^{7}G**5** c^{7}G**5**G)-3′	100; 97; 98	4
28	5′-d(GGG **555**)-3′	100; 100; 97	7
29	5′-d(**555** GGG)-3′	92; 94; 94	6
30	5′-d(c^{7}Gc^{7}Gc^{7}G **555**)-3′	100; 100; 98	5
31	5′-d(**1**G**1** G**1**G)-3′	100; 100; 95	13
32	5′-d(G**1**G **1**G**1**)-3′	100; 98; 96	12
33	5′-d(GGG **111**)-3′	100; 99; 98	3
34	5′-d(**111** GGG)-3′	95; 95; 95	4
35	5′-d(**1**c^{7}G**1** c^{7}G**1**G)-3′	100; 96; 97	6
36	5′-d(**555** **555**)-3′	90[a])	11
37	5′-d(**111** **111**)-3′	90[b])	16
38	5′-d(c^{7}G c^{7}G c^{7}G c^{7}G c^{7}G c^{7}G)-3′	96 – 100	8

[a]) Coupling yield of **10b**. [b]) Coupling yield of **7**.

Table 4. *Molecular Masses* [Da] *of Selected Oligodeoxynucleotides*

	M^+	
	calc.	found
5′-d(AGTATTGA**55**TA)-3′ (**21**)	3723	3726
5′-d(TAGGT**5**ATTA**5**T)-3′ (**22**)	3723	3722
5′-d(AGTATTGA**11**TA)-3′ (**23**)	3723	3722
5′-d(TAGGT**1**ATTA**1**T)-3′ (**24**)	3723	3728
5′-d(**5**G**5** G**5**G)-3′ (**25**)	1913	1913
5′-d(G**5**G **5**G**5**)-3′ (**26**)	1913	1912
5′-d(**5**c^{7}G**5**c^{7}G**5**G)-3′ (**27**)	1911	1915
5′-d(GGG **555**)-3′ (**28**)	1913	1916
5′-d(**555** GGG)-3′ (**29**)	1913	1912
5′-d(c^{7}Gc^{7}Gc^{7}G **555**)-3′ (**30**)	1910	1913
5′-d(**1**G**1** G**1**G)-3′ (**31**)	1913	1913
5′-d(G**1**G **1**G**1**)-3′ (**32**)	1913	1912
5′-d(GGG **111**)-3′ (**33**)	1913	1912
5′-d(**111** GGG)-3′ (**34**)	1913	1919
5′-d(**1**c^{7}G**1** c^{7}G**1**G)-3′ (**35**)	1911	1914
5′-d(**555** **555**)-3′ (**36**)	1913	1916
5′-d(**111** **111**)-3′ (**37**)	1913	1913

deoxyisoguanosine (**6**; iG_d) and all C_d units by 2′-deoxy-5-methylisocytidine (**4**; m^5iC_d) [7]. Thus, the reversal of the strand orientation is achieved by a transposition of substituents, thereby changing the donor-acceptor pattern of the bases. A second possibility to invert the strand orientation has been realized by changing the

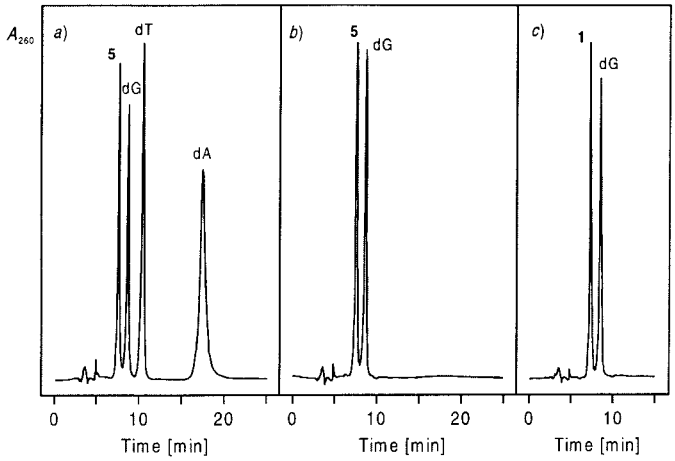

Figure. *Reversed-phase HPLC* (*RP-18*) *profiles of the reaction products obtained after enzymatic hydrolysis of the oligonucleotides* a) **21**, b) **25**, *and* c) **32** *by snake-venom phosphodiesterase at 37° after subsequent addition of alkaline phosphatase in* 1M Tris · *HCl buffer* (pH 8.3). Solvent system *III* for HPLC; for details, see *Exper. Part.*

Table 5. *Half-Life Values of Enzymatic Phosphodiester Hydrolysis of Oligodeoxyribonucleotides with Snake-Venom Phosphodiesterase* (SVPDE)[a])

	τ [min]		τ [min]
5′-d(**111 111**)-3′ **37**	1	[5′-d(G**1**G **1**G**1**)-3′]$_2$ **32** · **32**	8
5′-d(**555 555**)-3′ **36**	14	[5′-d(GCG CGC)-3′]$_2$ **39** · **39**	1
		[5′-d(G**5**G **5**G**5**)-3′]$_2$ **26** · **26**	20

[a]) Buffer: 0.1M *Tris* · HCl, pH 8.3; SVPDE, 3 μg/ml; 37°.

glycosylation position of the purine moiety from N(9) to N(7) within a purine · pyrimidine or a purine · purine base pair [22]. The third possibility to construct a parallel DNA is brought about by changing the anomeric configuration of the nucleotide building blocks of one strand from β-D to α-D [21][23]. A new variant is now opened up by using 5-aza-7-deazaguanine nucleosides: this base has the ability to act as a H-bond acceptor at N(1) analogous to 5-methylisocytosine (see base-pair motifs **I** and **II**) [6]. Thus, the β-D-anomer **1** forms a ps duplex, forming $(\beta)z^5c^7G_d$ (**1**) · $(\beta)G_d$ base pairs under neutral conditions (motif **I**). The strand polarity has been clearly shown by measuring the thermal stability of corresponding block oligomers [6][9]. On the other hand, with C_d compound **1** forms an aps strand under acidic conditions ($[(\beta)z^5c^7G_d$ (**1**) · $(\beta)C_d] \cdot H^+$; motifs **III** and **IV**) [6]. Moreover, it has been demonstrated [6] that the β-D-anomer **1** pairs in an antiparallel mode with 2′-deoxyisoguanosine (**6**; iG_d), similar to an $iG_d \cdot m^5iC_d$ (**4**; 2′-deoxy-5-methylisocytidine) base pair (motifs **V** and **VI**), but with a larger distance between the anomeric centers (C(1′) ··· C(1′) ≈ 13 Å) [24]. These results imply that compound **1** is prone to form 'purine' · purine base pairs, whereby their orientation (ps or aps) can be defined by the H-bond donor-acceptor pattern of the binding partner (guanine or isoguanine).

When changing the anomeric configuration from β-D (**1**) to α-D (**5**), the base pairs containing (β)z^{5}c^{7}G$_d$ (**1**) should again change their orientation when **1** is replaced by the α-D anomer **5**.

2.2.1. *Self-Complementary and Non-Selfcomplementary Hexamers.* In a first series of experiments, alternating self-complementary oligonucleotide hexamers were constructed, which were build up from **5** or **1** together with either 2′-deoxyguanosine (**2**) or

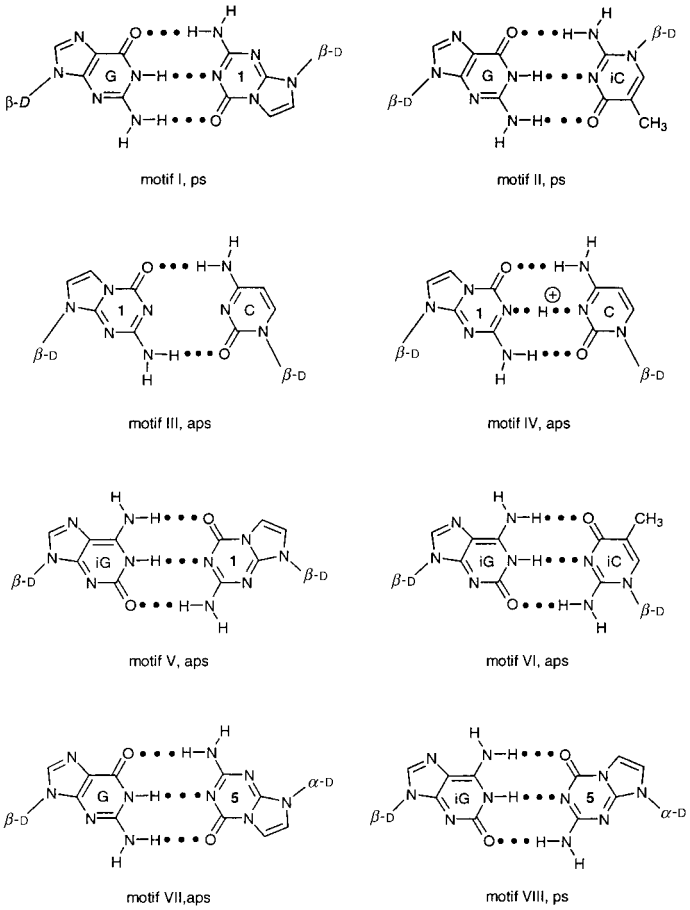

α-D = 2′-deoxy-α-D-ribofuranosyl; β-D = 2′-deoxy-β-D-ribofuranosyl

its 7-deazapurine analogue **3**. The incorporation of **5** led to an alternation of the anomeric configuration as well as of the donor-acceptor pattern of the bases along the same strand (*Table 6*, *Entry 1*; motifs **VII** and **VIII**). According to the structures of **1** and **5**, the hybridization should lead to all-'purine' duplexes.

The α-D- and β-D-nucleosides **5** or **1** together with **2** or **3** were also arranged in a consecutive way (*Table 6*, *Entry 2*). These block oligomers formed the same base pairs as the alternating ones; however, the configuration of the anomeric centers changes only once along the oligonucleotide chain. Moreover, aps- as well as ps-oriented

Table 6. *Schematic Assembly of Conceivable Hexamer Duplexes* (aps and ps) *Containing the Nucleoside Residues* **1** (*β*-D) *or* **5** (*α*-D)[a])

Entry	Oligomers described	Base pair (aps)	Oligomer described	Base pair (ps)
1	**25**·**25**; **26**·**26**; **27**·**27**	5′-d(*α*-*β*-*α*-*β*-*α*-*β*)-3′ 3′-d(*β*-*α*-*β*-*α*-*β*-*α*)-5′	–	5′-d(*α*-*β*-*α*-*β*-*α*-*β*)-3′ 5′-d(*β*-*α*-*β*-*α*-*β*-*α*)-3′
2	**28**·**28**; **29**·**29**; **30**·**30**	5′-d(*α*-*α*-*α*-*β*-*β*-*β*)-3′ 3′-d(*β*-*β*-*β*-*α*-*α*-*α*)-5′	–	5′-d(*α*-*α*-*α*-*β*-*β*-*β*)-3′ 5′-d(*β*-*β*-*β*-*α*-*α*-*α*)-3′
3	**36**·**38**	5′-d(*α*-*α*-*α*-*α*-*α*-*α*)-3′ 3′-d(*β*-*β*-*β*-*β*-*β*-*β*)-5′	–	5′-d(*α*-*α*-*α*-*α*-*α*-*α*)-3′ 5′-d(*β*-*β*-*β*-*β*-*β*-*β*)-3′
4	–	5′-d(*α*-*α*-*α*-*α*-*α*-*α*)-3′ 3′-d(*α*-*α*-*α*-*α*-*α*-*α*)-5′	–	5′-d(*α*-*α*-*α*-*α*-*α*-*α*)-3′ 5′-d(*α*-*α*-*α*-*α*-*α*-*α*)-3′
5	**33**·**43**	5′-d(*β*-*β*-*β*-*β*-*β*-*β*)-3′ 3′-d(*β*-*β*-*β*-*β*-*β*-*β*)-5′	**31**·**31**; **32**·**32**; **34**·**34**; **35**·**35**; **37**·**38**	5′-d(*β*-*β*-*β*-*β*-*β*-*β*)-3′ 5′-d(*β*-*β*-*β*-*β*-*β*-*β*)-3′

[a]) Note that not each possible oligomer assembly has been realized.

homomeric duplexes are conceivable (*Table 6*, *Entry 3*) and are now disclosed. Until today, oligonucleotide duplexes containing *α*-D- and *β*-D-configurated nucleoside residues within the same strand were found to be only stable when the chain orientation in this strand was also changed [25]. For all these duplexes, T_m values, shown in *Tables 7* and *8*, were measured (60 mM Na-cacodylate, 100 mM $MgCl_2$, 1M NaCl, pH 7), and the thermodynamic data of duplex formation were calculated from each individual melting

Table 7. T_m *Values and Thermodynamic Data of Alternating Self-Complementary Hexamers*[a])

Oligomer	T_m [°C]	Base pairs	$\Delta H°$ [kcal/mol]	$\Delta S°$ [cal/K mol]	$\Delta G°_{310}$ [kcal/mol]
5′-d(**5**G**5**G**5**G)-3′ **25** 3′-d(G**5**G**5**G**5**)-5′ **25**	63	6	– 70.0	– 185.6	– 12.4
5′-d(G**5**G**5**G**5**)-3′ **26** 3′-d(**5**G**5**G**5**G)-5′ **26**	56	6	– 52.4	– 136.4	– 10.1
5′-d(**5**c^{7}G **5** c^{7}G **5** G)-3′ **27** 3′-d(G **5** c^{7}G **5** c^{7}G**5**)-5′ **27**	53	6	– 53.8	– 140.7	– 10.2
5′-d(GCGCGC)-3′ **39** 3′-d(CGCGCG)-5′ **39**	46	6	– 54.9	– 150.0	– 8.4
5′-d(CGCGCG)-3′ **40** 3′-d(GCGCGC)-5′ **40**	44	6	– 50.8	– 139.0	– 7.7
5′-d(G**1**G**1**G**1**)-3′ **32** 5′-d(G**1**G**1**G**1**)-3′ **32**	*ca.* 55[b])	5	n.d.	n.d.	n.d.
5′-d(**1**G**1**G**1**G)-3′ **31** 5′-d(**1**G**1**G**1**G)-3′ **31**	55	5	– 53.4	– 149.6	– 10.1
5′-d(**1**c^{7}G**1**c^{7}G**1**G)-3′ **35** 5′-d(**1**c^{7}G**1**c^{7}G**1**G)-3′ **35**	54	5	– 54.9	– 145.4	– 9.8
5′-d(iCGiCGiCG)-3′ **42** 5′-d(iCGiCGiCG)-3′ **42**	21	5	n.d.	n.d.	n.d.

[a]) For details, see *Table 9*. [b]) Low cooperativity.

Table 8. T_m *Values and Thermodynamic Data of Self-Complementary Block Hexamers*[a])

	T_m [°C]	Base pairs	ΔH° [kcal/mol]	ΔS° [cal/K mol]	ΔG°_{310} [kcal/mol]
5′-d(GGGCCC)-3′ **41** 3′-d(CCCGGG)-5′ **41**	36	6	– 41	– 112	– 7
5′-d(GGG**5 5 5**)-3′ **28** 3′-d(**5 5 5**GGG)-5′ **28**	45	6	– 33.4	– 82.7	– 7.8
5′-d(**5 5 5**GGG)-3′ **29** 3′-d(GGG**5 5 5**)-5′ **29**	56	6	– 50.6	– 131.3	– 9.9
5′-d(c^{7}Gc^{7}Gc^{7}G **5 5 5**)-3′ **30** 3′-d(**5 5 5** c^{7}Gc^{7}Gc^{7}G)-5′ **30**	*ca.* 43[b])	6	n.d.	n.d.	n.d.
5′-d(GGG**1 1 1**)-3′ **33** 3′-d(CCCiGiGiG)-5′ **43**	47	6	– 75.7	– 212.9	– 9.7
5′-d(**1 1 1**GGG)-3′ **34** 3′-d(iGiGiGCCC)-5′ **44**	46	6	– 74.3	– 209.0	– 9.5
5′-d(**1 1 1**GGG)-3′ **34** 5′-d(**1 1 1**GGG)-3′ **34**	26	3	– 48.6	– 140.9	– 4.9
5′-d(**111111**)-3′ **37** 5′-d(**333333**)-3′ **38**	42	6	– 51.4	– 136.6	– 9.1
5′-d(**555555**)-3′ **36** 3′-d(**333333**)-5′ **38**	37	6	– 30.2	– 72.7	– 7.7

[a]) For details, see *Table 8*. [b]) Low cooperativity.

curve according to a two-state (duplex ⇔ random coil) model with the program MeltWin (release version 3.0) [26] (*Tables 7* and *8*).

The alternating hexamers [5′-d(**5**G**5** G**5**G)-3′]$_2$ (**25**·**25**) and [5′-d(G**5**G **5**G**5**)-3′]$_2$ (**26**·**26**) exhibit T_m values (*Table 7*) that are 10–13° higher than those of the parent oligomers [5′-d(CGCGCG)-3′]$_2$ (**40**·**40**) [27] and [5′-d(GCGCGC)-3′]$_2$ (**39**·**39**). However, in contrast to the latters, **25**·**25** and **26**·**26** differ in their T_m values significantly (ΔT_m 7°); they exhibit an antiparallel chain orientation as described above (base-pair motif **VII**). For comparison, also the alternating oligonucleotides containing the β-D-anomer **1** (**31**·**31**, **32**·**32**) instead of the α-D-anomer **5** were synthesized, and their T_m values were measured (*Table 7*). They exhibit T_m values higher than 50°, regardless of the fact that these duplexes (**31**·**31**, **32**·**32**) may be hold together by only five three-dentate base pairs with parallel orientation. The cooperativity of their melting curves is low. The rather high T_m values (*ca.* 55°) are partly due to a stabilizing effect of the dangling nucleotides (G_d and **1**, resp.) on both termini, thereby compensating the lower number of H-bonds (15) compared to the corresponding duplexes **25**·**25** and **26**·**26** (18 H-bonds).

Also the block oligomers 5′-d(GGG**555**)-3′ (**28**) and 5′-d(**555**GGG)-3′ (**29**) were prepared. They formed antiparallel, blunt-ended duplexes with themselves, showing significantly different T_m values ($\Delta T_m = 11°$, *Table 8*). If the oligomers **28** and **29** would have formed parallel-oriented duplexes, these should be hold together by only three base pairs – and not by five – which would most probably result in low T_m values. In this context, it is worth mentioning that the block oligomers **33** and **34** – both containing the β-D-anomer **1** – form self-complementary parallel duplexes with themselves, which are

hold together by only three (β)z^{5}c^{7}G$_d$ · G$_d$ base pairs, thereby exhibiting T_m values of 20 and 26°, respectively [6]. The high T_m values found, however, imply the formation of six reverse *Watson-Crick* (α)z^{5}c^{7}G$_d$ · G$_d$ base pairs with three H-bonds each. To the best of our knowledge, compounds **25**, **26**, **28**, and **29** are the first chimeric oligomers built-up from both, α-D- and β-D-anomeric nucleotide units, which are connected by regular 3′-5′-phosphodiester bonds, and which form duplex structures. Until today [25], such chimeric oligonucleotides have been constructed with alternating 3′-3′ and 5′-5′ phosphodiester bonds.

Next, the base-pairing properties of oligonucleotides containing the β-D-anomeric compound **1** with oligonucleotides incorporating the β-D-anomeric 2′-deoxyisoguanosine (**6**) was studied. Hybridization of 5′-d(GGG**111**)-3′ (**33**) or 5′-d(**111**GGG)-3′ (**34**) with 5′-d(CCCiGiGiG)-3′ (**44**) or 5′-d(iGiGiGCCC)-3′ (**43**), respectively (*Table 8*), resulted in the formation of fully matched antiparallel duplexes. These duplexes exhibit T_m values of 47 and 46°, respectively, which are 10 – 11° higher than that of the corresponding unmodified aps duplex [5′-d(GGGCCC)-3′]$_2$ (**41** · **41**; T_m 36°) containing 2′-deoxycytidine.

The results discussed above were confirmed by melting experiments with alternating as well as block oligomers containing 7-deaza-2′-deoxyguanosine (**3**; c^{7}G$_d$) instead of 2′-deoxyguanosine (**2**) (**27** · **27**, **30** · **30**, **35** · **35**; *Tables 7* and *8*). In these duplexes, *Hoogsteen* base pairing is excluded in both strands. The self-complementary aps duplex **27** · **27** ([5′-d(**5**c^{7}G**5**c^{7}G**5**G)-3′]$_2$) shows a T_m value of 53°, which is still 9° higher than that of the parent oligomer [5′-d(CGCGCG)-3′]$_2$ (**40** · **40**, T_m 44°; *Table 7*). The finding that, on the other hand, **27** · **27** exhibits a T_m value which is 10° lower than that of duplex **25** · **25** ([5′-d(**5**G**5**G**5**G)-3′]$_2$) can be traced back to the fact that **27** · **27** contains 3′-terminal G$_d$ residues instead of c^{7}G$_d$. Also the parallel duplex **35** · **35** ([5′-d(**1**c^{7}G**1**c^{7}G**1**G)-3′]$_2$) with a five-base-pair core of (β)z^{5}c^{7}G$_d$ · c^{7}G$_d$ but with different one-base overhangs (**1**, G$_d$) on the termini exhibits a high T_m value (54°) that is only 1° lower than that of the ps duplex **31** · **31** (*Table 7*). The antiparallel duplex **30** · **30** ([5′-d(c^{7}Gc^{7}Gc^{7}G**555**)-3′]$_2$) (*Table 8*) exhibits a melting curve with low cooperativity, which resists the evaluation of thermodynamic data of duplex formation, but allows at least an estimation of a T_m value (*ca.* 43°). This value is similar to that of **28** · **28** (45°) but significantly higher (ΔT_m 7°) than that of [5′-d(GGGCCC)-3′]$_2$ (**41** · **41**; T_m 36°).

Finally, the homomeric duplexes 5′-d(**111111**)-3′ · 5′-d(**333333**)-3′ (**37** · **38**) and 5′-d(**555555**)-3′ · 3′-d(**333333**)-5′ (**36** · **38**) were analyzed with respect to their thermal stability. The reason why oligo(7-deazaguanylic acid) (**38**) and not the corresponding purine oligomer was chosen as complementary strand is the strong self-aggregation of the latter. Due to the results described above, duplex **37** · **38** exhibits a parallel-strand orientation and **36** · **38** an antiparallel arrangement. As *Table 8* shows, these duplexes differ in their T_m values by 5°; the homochiral oligomer **37** · **38** exhibits the higher T_m value (42°) despite the fact that it is a parallel-stranded duplex. Considering the results described above, one can summarize that, within alternating or block oligonucleotides, the α-D-anomer **5** of 5-aza-7-deaza-2′-deoxyguanosine forms antiparallel, three-dentate heterochiral base pairs with G$_d$ (**2**) as well as with c^{7}G$_d$ (**3**). The β-D-anomer **1** forms parallel, three-dentate homochiral base pairs with G$_d$ and c^{7}G$_d$, and antiparallel pairs with 2′-deoxyisoguanosine (**6**).

2.2.2. *Non-Self-Complementary Oligonucleotide Duplexes.* To study the base-pairing properties of the anomers **1** and **5** within oligonucleotides with random nucleoside composition, they were incorporated in place of C_d into the *antiparallel* duplex **19**·**20** [28] as well as into the *parallel*-oriented duplexes **19**·**48**, **49**·**20**, and **50**·**51** [7][22] (*Table 9*). It was anticipated that an antiparallel **5**(α)·G_d(β) base pair would

Table 9. T_m *Values and Thermodynamic Data of Non-Self-Complementary Duplexes with Antiparallel and Parallel Strand Orientation*[a])

	T_m [°C]	ΔH° [kcal/mol]	ΔS° [cal/K mol]	ΔG°_{310} [kcal/mol]
5′-d(TAGGTCAATACT)-3′ **20** 3′-d(ATCCAGTTATGA)-5′ **19**	51	−84.9	−236.5	−11.6
5′-d(TA**GG**TCAATACT)-3′ **20** 3′-d(AT**5 5**AGTTATGA)-5′ **21**	38	−66.2	−187.5	−8.1
5′-d(TAGGT**5**AATA**5**T)-3′ **22** 3′-d(ATCCA**G**TTAT**G**A)-5′ **19**	26	−50.4	−142.9	−6.1
5′-d(A**G**TATT**G**A**5 5**TA)-3′ **21** 3′-d(T**5**ATAA**5**T**GG**AT)-5′ **22**	17	−40.4	−113.2	−5.3
5′-d(TAGGTCAATACT)-3′ **20** 3′-r(AUCCAGUUAUGA)-5′ **45**	48	−65	−176	−10.4
5′-d(TAGGT**5**AATA**5**T)-3′ **22** 3′-r(AUCCA**G**UUAU**G**A)-5′ **45**	30	−66.1	−192.0	−6.6
5′-d(TA**iGiG**TCAATACT)-3′ **46** 3′-d(AT**1 1**AGTTATGA)-5′ **23**	49	−82.8	−231.8	−10.9
5′-d(TAGGT**1**AATA**1**T)-3′ **24** 3′-d(ATCCA**iG**TTATi**G**A)-5′ **47**	48	−81.6	−229.1	−10.6
5′-d(AGTATTGACC TA)-3′ **19**[b]) 5′-d(TiCATAAiCTiGiGAT)-3′ **48**	44	−85.0	−242.0	−10.0
5′-d(ATiCiCAiGTTATiGA)-3′ **49**[b]) 5′-d(TAGGTCAATACT)-3′ **20**	39	−74.3	−212.3	−8.5
5′-d(AGTATTGAiCiCTA)-3′ **50**[c]) 5′-d(TiCATAAiCTGGAT)-3′ **51**	36	−70.2	−201.4	−7.8
5′-d(AGTATTGA**5 5**TA)-3′ **21** 5′-d(TiCATAAiCT**iGiG**AT)-3′ **48**	44	−74.0	−208.2	−9.5
5′-d(ATiCiCA**iG**TTATi**G**A)-3′ **49** 5′-d(TAGGT**5**AATA**5**T)-3′ **22**	39	−61.9	−173.5	−8.1
5′-d(AGTATTGA**1 1**TA)-3′ **23** 5′-d(TiCATAAiCT**GG**AT)-3′ **51**	40	−73.8	−210.0	−8.7
5′-d(ATiCiCA**G**TTAT**G**A)-3′ **52** 5′-d(TAGGT**1**AATA**1**T)-3′ **24**	44	−80.7	−229.1	−9.7

[a]) Measured at 260 nm in 1M NaCl, 100 mM $MgCl_2$, and 60 mM Na-cacodylate (pH 7) with 5 μM + 5 μM of single-strand concentration. Thermodynamic data were derived from the fitting of melting curves measured at 260 nm. The ΔG° values were calculated with the program MeltWin 3.0 referring to 310 K. Previously published results from our laboratory were obtained with the same program and refer to the same temperature, and not to 298 K as indicated. Thermodynamic data determined from *van't Hoff* plots with concentration-dependent T_m values were consistent with those obtained from curve fitting within 15%. The *van't Hoff* data for the formation of the duplex **20**·**19** in the above mentioned buffer are as follows: $\Delta H^\circ = -96.2$ kcal/mol, $\Delta S^\circ = -270.3$ cal/K mol, $\Delta G^\circ_{310} = -12.4$ kcal/mol. [b]) See [7]. [c]) See [22].

fit almost unconstrained into the duplex **20**·**19**. However, the replacement of two consecutive C_d residues within the oligomer **19** by the α-D-anomer **5** residues and hybridization with **20** resulted in an antiparallel duplex **20**·**21**, which exhibits a significantly lower T_m value than its unmodified counterpart **19**·**20** (ΔT_m −13°, *Table 9*). This T_m decrease became even more evident (ΔT_m −25°), when two C_d residues not in a row but in a distant position (see **20**) were replaced by **5**, and when the resulting modified single strand **22** was hybridized to **19**. After replacement of all C_d residues of **19**·**20** by **5**, the resulting duplex **21**·**22** exhibits a T_m value of merely 17° (ΔT_m −34°). Moreover, the heteroduplex **22**·**45** obtained by hybridazation of oligomer **22** containing two **5** residues with the complementary RNA strand **45** shows a T_m value that is 17° lower than that of the unmodified RNA·DNA duplex **20**·**45**.

These findings may be due to two different reasons: *i*) The incorporation of a 'purine'·purine base pair such as **5**(α)·G_d(β) with an extended C(1′)···C(1′) distance (*ca.* 13 Å) into an oligomer with otherwise purine·pyrimidine base pairs renders the DNA double helix non-isomorphic as it contains buldged-out regions. *ii*) On the basis of *Dreiding* stereomodels, *Sequin* [29] postulated, already in 1973, the existence of a parallel DNA duplex, built up from heterochiral α-D- and β-D-single strands. On the other hand, an antiparallel DNA duplex can be formed from two α-D-configurated strands. Additionally, it was anticipated that the formation of an antiparallel or parallel DNA double helix from single strands containing both α-D- and β-D-configurated nucleotide units is impossible. If, therefore, heterochiral base pairs are incorporated into a DNA duplex, the base pairs of which are predominantly homochiral, then the duplex structure becomes heteromorphous, and its thermal stability should decrease.

To decide what kind of heteromorphism exerts the highest influence on the thermal duplex stability, the *parallel*-stranded duplex **19**·**48** was synthesized. Upon the replacement of two parallel, homochiral C_d·iG_d base pairs by the heterochiral 'purine'·purine pair **5**(α)·iG_d(β), a duplex **21**·**48** was formed, which shows the same T_m value as **19**·**48** (44°). An analogous result was found for the pair of duplexes **49**·**20** and **49**·**22** (T_m 39°, each). Thus, different to duplexes with antiparallel chain orientation, the base pair **5**(α)·iG_d(β) is well-accommodated in a ps-duplex structure. In a further set of experiments, the β-D-anomer **1** was incorporated – in place of C_d or iC_d – into non-selfcomplementary random oligodeoxyribonucleotides opposite to either G_d (**2**) or iG_d (**6**) (see **46**·**23**, **24**·**47**, **23**·**51**, **52**·**24**). *Table 9* contains the T_m values as well as thermodynamic data of duplex formation. As can be seen, the incorporation of homochiral 'purine'·purine (β)**1**·(β)G_d base pairs into the parallel-oriented oligomer duplexes **23**·**51** and **52**·**24** even enhances the T_m value slightly (ΔT_m 4–5°), compared to the parent duplexes **50**·**51** and **49**·**20**, respectively. This means that, within parallel-stranded oligonucleotides, homochiral but bulged-out 'purine'·purine base pairs are tolerated. The same is true for antiparallel-oriented duplexes containing homochiral antiparallel (β)$z^5c^7G_d$·(β)iG_d base pairs such as **46**·**23** and **24**·**47** (*Table 9*); the T_m values amount to 49 and 48°, respectively, being close to that of the unmodified duplex **20**·**19** (T_m 51°).

3. Conclusion. – The following conclusion can be drawn from the above discussed results: *i*) Oligonucleotide duplexes that are built up exclusively from 'purine' nucleosides (*Tables 7* and *8*) adopt obviously isomorphic structures, which exhibit high

thermal stability. The latter is tendentiously higher than that of corresponding oligomers formed from purine · pyrimidine base pairs – a fact that can be due to better stacking interactions of the purine bases. *ii*) Parallel as well as antiparallel DNA duplexes incorporating heterochiral α-D-/β-D-base pairs are stable if the oligomer is syndiotactic with respect to the sequence or if it contains isotactic base tracts. *iii*) The incorporation of β-D-/β-D-configurated 'purine' · purine nucleotide base pairs into parallel- or antiparallel-oriented DNA duplexes with random base composition (*Table 9*) is tolerated. *iv*) The incorporation of even single heterochial α-D-/β-D-configurated purine · purine nucleotide base pairs into an otherwise isomorphic, antiparallel B-DNA leads to an atactic oligomer with the consequence of significantly decreased thermal stability. *v*) If, however, one or two heterochiral α-D-/β-D-configurated base pairs are incorporated into a parallel DNA duplex, the stability of the resulting atactic duplex is retained. In particular, the last result is enigmatic as it opposes apparently the prognosis of *Sequin* [29] concerning the stability of such DNA molecules.

Experimental Part

General. All chemicals were purchased from *Aldrich*, *Sigma*, or *Fluka* (*Sigma-Aldrich Chemie GmbH*, Deisenhofen, Germany). Solvents were of laboratory grade and were distilled before use. Thin-layer chromatography (TLC): aluminium sheets, silica gel *60* F_{254}, 0.2 mm layer (*Merck*, Germany). Column flash chromatography (FC): silica gel *60* (*Merck*, Germany) at 0.5 bar ($4 \cdot 10^4$ Pa); sample collection with an *UltroRac-II* fractions collector (*LKB Instruments*, Bromma, Sweden). Melting points: *Büchi SMP-20* apparatus (*Büchi*, Switzerland); uncorrected. UV Spectra: *U-3200*-UV/VIS spectrometer (*Hitachi*, Japan). CD Spectra: *Jasco 600* spectropolarimeter (*Jasco*, Tokio, Japan), with a temp. controller *Lauda RCS 6* and a water bath *Lauda RK 20* (*Lauda* Germany); 1-cm cuvettes. NMR Spectra: *Avance DPX-250* or *AMX-500* spectrometers (*Bruker*, Germany) at 250.13 and 500.14 MHz (^{1}H), at 125.13 (^{13}C) and 101.3 MHz (^{31}P); chemical shifts δ are in ppm rel. to $SiMe_4$ as internal standard or external 85% H_3PO_4. *J* values in Hz. MALDI-TOF-MS were recorded by Dr. *Thomas Wenzel*, *Bruker Saxonia Analytik GmbH*, Leipzig. Elemental analyses were performed by *Mikroanalytisches Laboratorium Beller* (Göttingen, Germany).

Oligonucleotide Synthesis. The oligodeoxyribonucleotides were synthesized with a DNA synthesizer, model *382* (*Applied Biosystems*, Weiterstadt, Germany), on a 1-μmol scale. Most of the syntheses followed the regular protocol of the DNA synthesizer for phosphoramidites [22]. After cleavage from the solid support, the oligonucleotides were deprotected in 25% aq. NH_3 soln. for 12–16 h at 60°. The oligomers **36** and **37** were prepared from the phosphonates **7** and **10b** according to a slightly modified protocol of the DNA synthesizer (*Applied Biosystems, ABI 392*) for 3′-phosphonates [19] with *Universal CPG* columns carrying a 3′-terminal ribose moiety (*Glen Research*, Sterling, VA, USA). The coupling time for the modified 3′-phosphonates was prolonged to 2×120 s, and the capping time was trebled to 90 s. As the 3′-phosphonate **10b** proved less soluble in MeCN compared to **7**, its concentration was halved and the mixture ultra-sonicated for 45 min before use. In the latter case, cleavage of the oligomers (5′-$(MeO)_2$Tr-**37**, 5′-$(MeO)_2$Tr-**38**) from the support was performed with conc. aq. NH_3 soln. in the presence of LiCl (2.2%, *w*/*v*) at 55° (16 h). Results: *Table 3*.

Oligomer Hydrolysis. The enzymatic hydrolysis of all oligomers with snake-venom phosphodiesterase (EC 3.1. 15.1, *Crotallus durissus*) and alkaline phosphatase (EC 3.1.3.1, *E. coli*) was carried out as described in [20]. The mixture was analyzed on reversed-phase HPLC (*RP-18*, solvent system *III*). Quantification of the resulting nucleosides was made on the basis of the peak areas, which were divided by the extinction coefficients of the nucleoside constituents at λ 260 nm: A_d 15400, C_d 7300, G_d 11700, T_d 8800, $c^7z^5G_d$ 11500.

HPLC Separation. HPLC was carried out according to [24]. Eluents: 0.1M (Et_3NH)OAc, pH 7.0/MeCN 95 : 5 (*A*) and MeCN (*B*); Gradient *I:* 30 min 5–40% *B* in *A*; 10 min 50% *A* in *B*; 5 min *A*, flow rate 1 ml/min Gradient *II:* 30 min 0–20% *B* in *A*; 10 min 25% *B* in *A*; 5 min 5% *A*, flow rate 1 ml/min. Gradient *III:* 20 min *A*, flow rate 0.6 ml/min.

Melting Experiments. The thermal dissociation/association of the duplexes was measured by temp.-dependent UV-melting profiles with a *Cary-1E* UV/VIS spectrophotometer (*Varian*, Australia) equipped with a *Cary* thermoelectrical controller; the actual temp. was measured in the reference cell with a Pt-100 resistor. The thermodynamic data of duplex formation were calculated using the program MeltWin [26].

*2-Amino-8-[2′-deoxy-5′-*O*-(4,4′-dimethoxytrityl)-α-*D*-erythro-pentofuranosyl]imidazo[1,2-a]-1,3,5-triazin-(8H)-one* (**10a**). Compound **5** (1.62 g, 6.09 mmol) was dried by repeated co-evaporation from anh. pyridine and then dissolved in anh. pyridine (2 ml). After addition of 4,4′-dimethoxytrityl chloride ($(MeO)_2TrCl$; 1.87 g, 5.5 mmol) under Ar, the soln. was stirred for 3.5 h at r.t. After addition of 5% aq. $NaHCO_3$ soln. (300 ml), the mixture was extracted twice with CH_2Cl_2 (200 ml) and the combined org. extract dried (Na_2SO_4), and evaporated. FC (column 22×1.8 cm, CH_2Cl_2/MeOH/Et_3N 88:10:2 (100 ml), then CH_2Cl_2/MeOH/Et_3N 78:20:2) afforded **10a** (1.9 g, 54%). Colorless, amorphous solid. TLC (silica gel, CH_2Cl_2/MeOH 8:2): R_f 0.38. ^{1}H-NMR ((D_6)DMSO): 7.56 (*d*, $J = 2.8$, H–C(7)); 7.39 (*m*, H–C(6), 1 arom. H); 7.40 (*m*, 3 arom. H); 7.24 (*m*, NH_2, 3 arom. H); 6.92 (*m*, 6 arom. H); 6.27 (*dd*, $J(1',2'\beta) = 7.8$, $J(1',2'\alpha) = 7.9$, H–C(1′)); 5.58 (*d*, $J =$ 3.3, OH–C(3′)); 4.28 (br. *s*, H–C(3′), H–C(4′)); 3.73 (*s*, MeO); 3.13 (*m*, 1 H–C(5′)); 3.01 (*m*, 1 H–C(5′)); 2.73 (*m*, H_α–C(2′)); 2.19 (*m*, H_β–C(2′)). Anal. calc. for $C_{31}H_{31}N_5O_6$ (569.59): C 65.37, H 5.49, N 12.29; found: C 65.24, H 5.38, N 12.12.

*2-Amino-8-[2′-deoxy-5′-*O*-(4,4′-dimethoxytrityl)-α-*D*-erythro-pentofuranosyl]imidazo[1,2-a]-1,2,3-triazin-4(8H)-one 3′-(Triethylammonium Phosphonate)* (**10b**). To a soln. of PCl_3 (505 µl, 5.94 mmol) and *N*-methylmorpholine (6.4 ml), 57.2 mmol) in anh. CH_2Cl_2 (54 ml), 1*H*-1,2,4-triazole (1.32 g, 19.13 mmol) was added at r.t. After stirring for 30 min and cooling to 0°, a soln. of **10a** (640 mg, 0.4 mmol) in CH_2Cl_2 (33 ml) was added. After stirring for 20 min, the mixture was hydrolyzed by addition of 1M $(Et_3NH)HCO_3$ buffer (pH 7.5; 60 ml). The aq. phase was extracted with CH_2Cl_2 (3×40 ml), the combined org. extract dried (Na_2SO_4) and evaporated, and the residue submitted to FC (column 15×1.8 cm, CH_2Cl_2/MeOH 8:2 (100 ml) and 75:25 (100 ml), then CH_2Cl_2/MeOH/Et_3N 95:3:2). The main zone was evaporated and the residue dissolved in CH_2Cl_2 (40 ml) and extracted with 0.1M $(Et_3NH)HCO_3$ buffer. After drying (Na_2SO_4) and evaporation, **10b** (464 mg, 56%) was obtained as a yellowish foam. TLC (silica gel, CH_2Cl_2/MeOH 75:25): R_f 0.47. ^{1}H-NMR ($(D)_6$DMSO): 7.78 (*s*, 1/2 H, PH); 7.58 (*d*, $J = 2.7$, H–C(7)); 7.34 (*m*, H–C(6), 3 arom. H); 7.23 (*m*, NH_2, 4 arom. H); 6.90 (*m*, 6 arom. H); 6.28 (‘*t*’, H–C(1′)); 5.44 (*s*, 1/2 H, PH); 4.67 (*m*, H–C(3′)); 4.43 (*m*, H–C(4′)); 3.73 (*m*, MeO); 3.11 (*m*, 1 H–C(5′)); 3.00 (*m*, 1 H–C(5′)); 2.81 (*m*, 3 CH_2); 2.40 (*m*, H_α–C(2′)); 2.35 (*m*, H_β–C(2′)); 1.06 (*m*, 2 Me). ^{31}P-NMR ((D_6)DMSO): 1.43 (^1J(P,H) = 589.3, ^3J(P,H) = 8.27). Anal. calc. for $C_{37}H_{47}N_6O_8P$ (734.81): C 60.48, H 6.45, N 11.44; found: C 60.60, H 6.63, N 11.18.

*8-(2′-Deoxy-α-*D*-erythro-pentofuranosyl)-2-(dibenzoylamino)imidazo[1,2-a]-1,2,3-triazin-4(8H)-one* (**10c**). Compound **5** (100 mg, 0.37 mmol) was evaporated twice with anh. pyridine and then dissolved in dry pyridine (3 ml). Then, Me_3SiCl (450 µl, 3.6 mmol) was added under Ar. After stirring for 30 min at r.t., benzoyl chloride (200 µl, 1.7 mmol) was added, and stirring was continued for 3 h. After cooling to 0°, H_2O (1 ml), and after 10 min, 25% aq. NH_3 soln. (0.8 ml) were added. After stirring for another 30 min, the solvent was evaporated and the residue taken up in 5% aq. $NaHCO_3$ soln. (10 ml). This soln. was extracted twice with AcOEt (2×15 ml). The combined org. layer was dried (Na_2SO_4) and evaporated and the residue submitted to FC (column 15×2 cm, CH_2Cl_2/MeOH 95:5): **10c** (81 mg, 46%). Colorless foam. TLC (silica gel, CH_2Cl_2/MeOH 9:1): R_f 0.27. UV (MeOH): 275 (9000). ^{1}H-NMR ((D_6)DMSO): 7.85–7.48 (*m*, 12 arom. H, H–C(7), H–C(8)); 6.00 (‘*d*’, $J = 6.2$, H–C(1′)); 5.47 (*d*, $J = 3.1$, OH–C(3′)); 4.85 (*t*, $J = 5.6$, OH–C(5′)); 4.23 (*m*, H–C(3′)); 4.16 (*m*, H–C(4′)); 3.35 (*m*, 2 H–C(5′)); 2.74 (*m*, H_α–C(2′)); 1.87 (*m*, H_β–C(2′)). Anal. calc. for $C_{24}H_{21}N_5O_6$ (475.45): C 60.63, H 4.45, N 14.73; found: C 60.10, H 4.64, N 13.97.

*8-(2′-Deoxy-α-*D*-erythro-pentofuranosyl)-2-{[(dibutylamino)methylidene]amino}imidazo[1,2-a]-1,2,3-triazin-4(8H)-one* (**12a**). To a suspension of **5** (200 mg, 0.75 mmol) in MeOH (9 ml), dibutylformamide dimethyl acetal (0.5 ml, 2.38 mmol) was added. The mixture was stirred at 40° for 1 h (TLC monitoring) and then evaporated. The residue was applied to FC (silica gel, 15×3 cm, CH_2Cl_2/MeOH 95:5): **12a** (255 mg, 84%). Colorless foam. TLC (silica gel, CH_2Cl_2/MeOH 9:1): R_f 0.49. UV (MeOH): 304 (26400), 241 (8700). ^{1}H-NMR ((D_6)DMSO): 8.74 (*s*, NCHN); 7.69 (*d*, $J = 2.7$, H–C(7)); 7.46 (*d*, $J = 2.7$, H–C(8)); 6.35 (‘*d*’, $J = 6.6$, H–C(1′)); 5.62 (*d*, $J = 3.5$, OH–C(3′)); 4.88 (*t*, $J = 5.7$, OH–C(5′)); 4.31 (*m*, H–C(3′)); 4.13 (*m*, H–C(4′)); 3.41 (*m*, 2 H–C(5′)); 3.37 (*m*, 2 CH_2N); 2.78–2.67 (*m*, H_α–C(2′)); 2.17–2.12 (*m*, H_β–C(2′)); 1.53 (*m*, 2 CH_2CH_2N); 1.34–1.23 (*m*, 2 MeCH_2); 0.93–0.88 (*m*, 2 Me). Anal. calc. for $C_{19}H_{30}N_6O_4$ (406.48): C 56.14, H 7.44; found: C 55.91, H 7.55.

*8-(2′-Deoxy-α-*D*-erythro-pentofuranosyl)-2-{[(dimethylamino)ethylidene]amino}imidazo[1,2-a]-1,3,5-triazin-4(8H)-one* (**12b**). To a suspension of **5** (100 mg, 0.37 mmol) in MeOH (5 ml), *N*,*N*-dimethylacetamide dimethyl acetal (150 µl, 1 mmol) was added under stirring at 35°. Stirring was continued for 2 h. After evaporation, the residue was submitted to FC (silica gel, column 15×2 cm, CH_2Cl_2/MeOH 85:5): **12b** (64 mg, 51%). Colorless, amorphous solid. TLC (silica gel, CH_2Cl_2/MeOH 85:5): R_f 0.25. ^{1}H-NMR ((D_6)DMSO): 7.66 (*d*, $J = 2.6$, H–C(7)); 7.44 (*d*, $J = 2.6$, H–C(8)); 6.27 (‘*d*’, $J = 6.0$, H–C(1′)); 5.61 (*d*, $J = 3.3$, OH–C(3′)); 4.87

(t, J = 5.2, OH–C(5′)); 4.30 (m, H–C(3′)); 4.12 (m, H–C(4′)); 3.41 (m, H–C(5′)); 3.02 (s, Me_2N); 2.75–2.64 (m, H_α–C(2′)); 2.16–2.08 (m, H_β–C(2′), MeC).

*8-(2′-Deoxy-α-*D*-*erythro*-pentofuranosyl)-2-{[(diisobutylamino)methylidene]amino}imidazo[1,2-*a*]-1,2,3-triazin-4(8*H*)-one* (**12c**). A soln. of **5** (50 mg, 0.19 mmol) in DMF (3 ml) was stirred with diisobutylformamide dimethyl acetal (0.4 ml, 1.91 mmol) for 24 h at 70°. After evaporation, the residue was applied to FC (silica gel, 20 × 2 cm, CH_2Cl_2/MeOH 9:1): **12c** (15 mg, 20%). Yellow foam. TLC (silica gel, CH_2Cl_2/MeOH 9:1): R_f 0.34. ^{1}H-NMR ((D$_6$)DMSO): 8.79 (s, NCHN); 7.71 (d, J = 2.7, H–C(7)); 7.45 (d, J = 2.6, H–C(8)); 6.34 ('d', J = 6.6, H–C(1′)); 5.65 (m, OH–C(3′)); 4.91 (m, OH–C(5′)); 4.31 (m, H–C(3′)); 4.13 (m, H–C(4′)); 3.35 (m, 2 H–C(5′), 2 Me_2CHCH_2); 2.69 (m, 2 Me_2CHCH_2); 2.18–1.98 (m, 2 H–C(2′)); 0.89 (m, 2 Me_2CHCH_2).

*8-(2′-Deoxy-α-*D*-*erythro*-pentofuranosyl)-2-{[(dimethylamino)methylidene]amino}imidazo[1,2-*a*]-1,2,3-triazin-4-(8*H*)-one* (**12d**). A suspension of **5** (100 mg, 0.37 mmol) in anh. MeOH (3 ml) was treated with dimethylformamide dimethyl acetal (250 µl, 1.88 mmol), stirred at r.t. for 5 h, and evaporated. The residue was adsorbed on silica gel and applied to FC (silica gel, column 20 × 2 cm, CH_2Cl_2/MeOH 85:15). Evaporation gave **12d** (84 mg, 70%). Amorphous solid. TLC (silica gel, CH_2Cl_2/MeOH 85:5): R_f 0.33. UV (MeOH): 301 (27200), 243 (9200). ^{1}H-NMR ((D$_6$)DMSO): 8.74 (s, NCHN); 7.69 (s, H–C(7)); 7.46 (s, H–C(8)); 6.34 ('d', J = 6.9, H–C(1′)); 5.62 (m, OH–C(3′)); 4.87 (d, J = 5.2, OH–C(5′)); 4.30 (m, H–C(3′)); 4.13 (m, H–C(4′)); 3.41 (m, 2 H–C(5′)); 3.15 (s, MeN); 3.02 (s, MeN); 2.75–2.67 (m, H_α–C(2′)); 2.17–2.12 (m, H_β–C(2′)). Anal. calc. for $C_{13}H_{18}N_6O_4$ (322.32): C 48.44, H 5.63; found: C 47.99, H 5.64.

*8-[2′-Deoxy-5′-*O*-(4,4′-dimethoxytrityl)-α-*D*-*erythro*-pentofuranosyl]-2-{[(dibutylamino)methylidene]amino}imidazo[1,2-*a*]-1,2,3-triazin-4(8*H*)-one* (**13**) *and 8-[2′-Deoxy-5′-*O*-(4,4′-dimethoxytrityl)-α-*D*-*erythro*-pentofuranosyl]-2-(formylamino)imidazo[1,2-*a*]-1,2,3-triazin-4(8*H*)-one* (**14**). Compound **12a** (450 mg, 1.11 mmol) was dried by repeated co-evaporation with anh. pyridine and suspended in dry pyridine (5 ml). The soln. was stirred under Ar in the presence of $(MeO)_2TrCl$ (510 mg, 1.51 mmol) for 3 h. Then, the mixture was diluted with a 5% aq. $NaHCO_3$ soln. (40 ml) and extracted with CH_2Cl_2 (3 × 30 ml). The combined org. phase was dried (Na_2SO_4) and evaporated, and the residue separated by FC (silica gel, column 15 × 3 cm, AcOEt/acetone 4:1): more polar **13** (613 mg, 78%) and less polar **14** (51 mg, 8%).

Data of **13**: Colorless amorphous solid. TLC (silica gel, AcOEt/acetone 4:1): R_f 0.15. UV (CH_2Cl_2): 304 (30200), 275 (16600), 236 (27300). ^{1}H-NMR ((D$_6$)DMSO): 8.73 (s, NCHN); 7.71 (d, J = 2.7, H–C(7)); 7.48 (d, J = 2.7, H–C(8)); 7.42–7.20 (m, 9 arom. H); 6.91 (m, 4 arom. H); 6.42 ('d', H–C(1′)); 5.67 (d, J = 3.4, OH–C(3′)); 4.28 (m, H–C(3′), H–C(4′)); 3.74 (s, 2 MeO); 3.50–3.42 (m, 2 CH_2N); 3.12, 2.99 (2m, 2 H–C(5′)); 2.87–2.72 (m, H_α–C(2′)); 2.24–2.18 (m, H_β–C(2′)); 1.58–1.49 (m, 2 CH_2CH_2N); 1.34–1.21 (m, 2 $MeCH_2$); 0.93–0.85 (m, 2 Me). Anal. calc. for $C_{40}H_{48}N_6O_6$ (708.85): C 67.78, H 6.83, N 11.86; found: C 68.34, H 7.05, N 11.43.

Data of **14**: Colorless foam. TLC (silica gel, AcOEt/acetone 4:1): R_f 0.29. UV (CH_2Cl_2): 276 (14400), 225 (36000). ^{1}H-NMR ((D$_6$)DMSO): 10.86 (d, J = 9.2, NH); 9.36 (d, J = 9.3, CHO); 7.80 (d, J = 2.7, H–C(7)); 7.60 (d, J = 2.7, H–C(8)); 7.41–7.21 (m, 9 arom. H); 6.93–6.86 (m, 4 arom. H); 6.39 ('d', H–C(1′)); 5.63 (d, J = 2.9, OH–C(3′)); 4.32 (m, H–C(3′), H–C(4′)); 3.74 (s, 2 MeO); 3.36, 3.12 (2m, 2 H–C(5′)); 2.82–2.70 (m, H_α–C(2′)); 2.28–2.21 (m, H_β–C(2′)). Anal. calc. for $C_{32}H_{31}N_5O_7$ (597.62): C 64.31, H 5.23; found: C 64.25, H 5.13.

*8-[2′-Deoxy-5′-*O*-(4,4′-dimethoxytrityl)-α-*D*-*erythro*-pentofuranosyl)]-2-(dibutylamino)methylidene]amino}imidazo[1,2-*a*]-1,2,3-triazin-4(8*H*)-one 3′-(2-Cyanoethyl Diisopropylphosphoramidite)* (**11**). To a soln. of **13** (270 mg, 0.38 mmol) and anh. ^{i}Pr$_2$EtN (100 µl, 0.56 mmol) in anh. CH_2Cl_2 (10 ml), 2-cyanoethyl diisopropylphosphor-amidochloridite (210 µl, 0.93 mmol) was added at r.t. under Ar. After stirring for 20 min, the mixture was diluted with CH_2Cl_2 (10 ml) and the reaction quenched by adding 5% aq. $NaHCO_3$ soln. (15 ml). Then, the aq. layer was extracted with CH_2Cl_2 (3 × 30 ml), the combined org. layer dried (Na_2SO_4) and evaporated, and the residual colorless oil applied to FC (silica gel, column 10 × 2 cm, CH_2Cl_2/acetone 6:4): **11** (252 mg, 83%). Colorless foam. TLC (silica gel, CH_2Cl_2/acetone 6:4): R_f 0.82, 0.73. ^{31}P-NMR ($CDCl_3$): 150.31; 150.17.

*8-(2′-Deoxy-β-*D*-*erythro*-pentofuranosyl)-2-{[(dibutylamino)methylidene]amino}imidazo[1,2-*a*]-1,2,3-triazin-4(8*H*)-one* (**15**). As described for the α-D-anomer **12a**, **1** (100 mg, 0.37 mmol) was treated with dibutylformamide dimethyl acetal (0.30 ml, 1.43 mmol). FC (silica gel, column 15 × 2 cm, CH_2Cl_2/MeOH 95:5) furnished **15**. Colorless foam (105 mg, 69%). TLC (silica gel, CH_2Cl_2/MeOH 9:1): R_f 0.44. UV (MeOH): 303 (26900), 245 (8900). ^{1}H-NMR ((D$_6$)DMSO): 8.93 (s, NCHN); 7.61 (d, J = 2.7, H–C(7)); 7.49 (d, J = 2.6, H–C(8)); 6.32 ('t', J = 6.8, H–C(1′)); 5.34 (d, J = 3.8, OH–C(3′)); 5.04 (t, J = 5.3, OH–C(5′)); 4.34 (m, H–C(3′)); 3.83 (m, H–C(4′)); 3.59 (m, 2 CH_2N); 3.41 (m, 2 H–C(5′)); 2.79–2.68 (m, H_α–C(2′)); 2.33–2.24 (m, H_β–C(2′)); 1.59–1.50 (m, 2 CH_2CH_2N); 1.35–1.23 (m, 2 $MeCH_2$); 0.94–0.86 (m, 2 Me). Anal. calc. for $C_{19}H_{30}N_6O_4$ (406.48): C 56.14, H 7.44, N 20.68; found: C 55.89, H 7.22, N 20.57.

8-[2′-Deoxy-5′-O-*(4,4′-dimethoxytrityl)-β*-D-erythro-*pentofuranosyl]-2-{[(dibutylamino)methylidene]amino}imidazo[1,2*-a*]-1,2,3-triazin-4(8*H*)-one* (**16**) *and 8-[2′-Deoxy-5′*-O-*(4,4′-dimethoxytrityl)-β*-D-erythro-*pentofuranosyl]-2-(formylamino)imidazo[1,2*-a*]-1,2,3-triazin-4(8*H*)-one* (**17**). As described for **13**/**14**, from **15** (300 mg, 0.74 mmol) and $(MeO)_2TrCl$ (450 mg, 1.33 mmol). FC (silica gel, column 10×3 cm, AcOEt/acetone 4:1): more polar **16** (310 mg, 59%) and less polar **17** (38 mg, 9%).

Data of **16**: Colorless amorphous solid. TLC (silica gel, AcOEt/acetone 4:1): R_f 0.13. UV (CH_2Cl_2): 305 (31200), 277 (16100), 237 (28300). ^{1}H-NMR ((D_6)DMSO): 8.73 (*s*, NCHN); 7.47 (*d*, $J = 2.6$, H–C(7)); 7.42 (*d*, $J = 2.7$, H–C(8)); 7.36–7.20 (*m*, 9 arom. H); 6.86–6.81 (*m*, 4 arom. H); 6.34 (‘*t*’, $J = 5.7$, H–C(1′)); 5.41 (*d*, $J = 4.7$, OH–C(3′)); 4.35 (*m*, H–C(3′)); 3.92 (*m*, H–C(4′)); 3.72 (*s*, 2 MeO); 3.51–3.41 (*m*, 2 CH_2N); 3.18–3.14 (*m*, 2 H–C(5′)); 2.71 (*m*, H_α–C(2′)); 2.36–2.28 (*m*, H_β–C(2′)); 1.59–1.53 (*m*, 2 CH_2CH_2N); 1.35–1.23 (*m*, 2 MeCH_2); 0.94–0.88 (*m*, 2 Me). Anal. calc. for $C_{40}H_{48}N_6O_6$ (708.85): C 67.78, H 6.83, N 11.86; found: C 67.97, H 6.89, N 11.68.

Data of **17**: Colorless foam. TLC (silica gel, AcOEt/acetone 4:1): R_f 0.27. UV (CH_2Cl_2): 277 (14000), 225 (36700). ^{1}H-NMR ((D_6)DMSO): 10.89 (*d*, $J = 8.7$, NH); 9.32 (*d*, $J = 8.9$, CHO); 7.63 (*d*, $J = 2.6$, H–C(7)); 7.54 (*d*, $J = 2.7$, H–C(8)); 7.35–7.19 (*m*, 9 arom. H); 6.86–6.81 (*m*, 4 arom. H); 6.29 (‘*t*’, $J = 6.0$, H–C(1′)); 5.40 (*d*, $J = 4.5$, OH–C(3′)); 4.38 (*m*, H–C(3′)); 3.94 (*m*, H–C(4′)); 3.73 (*s*, 2 MeO); 3.16 (*m*, 2 H–C(5′)); 2.57 (*m*, H_α–C(2′)); 2.32 (*m*, H_β–C(2′)). Anal. calc. for $C_{32}H_{31}N_5O_7$ (597.62): C 64.31, H 5.23, N 11.72; found: C 64.14, H 5.51, N 11.58.

8-[2′-Deoxy-5′-O-*(4,4′-dimethoxytrityl)-β*-D-erythro-*pentofuranosyl]-2-{[(dibutylamino)methylidene]amino}imidazo[1,2*-a*]-1,2,3-triazin-4(8*H*)-one 3′-(2-Cyanoethyl Diisopropylphosphoramidite)* (**18**). As described for **13**, **16** (320 mg, 0.45 mmol) was treated with 2-cyanoethyl diisopropylphosphoramidochloridite (150 µl, 0.67 mmol) and ^{i}Pr$_2$EtN (150 µl, 0.87 mmol). FC (silica gel, column 15×2 cm, CH_2Cl_2/acetone 6:4) furnished **18** (265 mg, 74%). Foam. TLC (silica gel, CH_2Cl_2/MeOH 6:4): R_f 0.83, 0.79. ^{31}P-NMR ($CDCl_3$): 150.02; 149.97.

We thank Mrs. *Elisabeth Feiling* for the oligonucleotide synthesis. Financial support by the *Deutsche Forschungsgemeinschaft* is gratefully acknowledged.

REFERENCES

[1] F. Seela, H. Rosemeyer, ‘5-Aza-7-deazapurines: Synthesis and Properties of Nucleosides and Oligonucleotides’, in ‘Recent Advances in Nucleosides: Chemistry and Chemotherapy’, Ed. D. C. K. Chu, Elsevier Press, 2001, in press; G. R. Revankar, R. K. Robins, ‘The Synthesis and Chemistry of Heterocyclic Analogues of Purine Nucleosides and Nucleotides’, in ‘Chemistry of Nucleosides and Nucleotides’, Vol. 2, Ed. L. B. Townsend, Plenum Press, New York, 1991, p. 161.
[2] H. Rosemeyer, F. Seela, *J. Org. Chem*. **1987**, *52*, 5136.
[3] H.-D. Winkeler, F. Seela, *J. Org. Chem*. **1983**, *48*, 3119.
[4] J. J. Voegel, M. M. Altorfer, S. A. Benner, *Helv. Chim. Acta* **1993**, *76*, 2061.
[5] J. J. Voegel, S. A. Benner, *Helv. Chim. Acta* **1996**, *79*, 1881.
[6] F. Seela, A. Melenewski, *Eur. J. Org. Chem*. **1999**, 485.
[7] F. Seela, C. Wei, *Helv. Chim. Acta* **1999**, *82*, 726.
[8] S.-H. Kim, D. G. Bartholomew, L. B. Allen, R. K. Robins, G. R. Revankar, P. Dea, *J. Med. Chem*. **1978**, *21*, 883.
[9] A. Melenewski, Thesis, University of Osnabrück, 1998.
[10] T. Wada, Y. Sato, F. Honda, S. Kawahara, M. Sekine, *J. Am. Chem. Soc*. **1997**, *119*, 12710.
[11] P. P. Kung, R. A. Jones, *Tetrahedron Lett*. **1992**, *33*, 5869.
[12] S. M. Gryaznov, R. L. Letsinger, *J. Am. Chem. Soc*. **1991**, *113*, 5876.
[13] G. S. Ti, B. L. Gaffney, R. A. Jones, *J. Am. Chem. Soc*. **1982**, *104*, 1316.
[14] J. Zemlička, A. Holy, *Coll. Czech. Chem. Commun*. **1967**, *32*, 3159.
[15] B. C. Froehler, M. D. Matteucci, *Nucleic Acids Res*. **1983**, *11*, 8031.
[16] H. Schaller, G. Weimann, B. Lerch, H. G. Khorana, *J. Am. Chem. Soc*. **1963**, *85*, 3821.
[17] S. L. Beaucage, M. H. Caruthers, *Tetrahedron Lett*. **1981**, *22*, 1859.
[18] B. C. Froehler, ‘Protocols of Oligonucleotides and Analogs’, in ‘Methods in Molecular Biology’, Ed. E. S. Agrawal, Humana Press, Tutowa, New Jersey, 1994, Vol. 20, p. 33.
[19] F. Seela, C. Wei, *Helv. Chim. Acta* **1997**, *80*, 73; ‘Users Manual of the DNA/RNA synthesizer, model 392’, Applied Biosystems.

[20] F. Seela, S. Lampe, *Helv. Chim. Acta* **1991,** *74*, 1790.
[21] F. Morvan, B. Rayner, J.-L. Imbach, S. Thenet, J.-R. Bertrand, J. Paoletti, C. Malvy, C. Paoletti, *Nucleic Acids Res.* **1987**, *15*, 3421.
[22] F. Seela, P. Leonard, *Helv. Chim. Acta* **1998**, *81*, 2244.
[23] F. Morvan, B. Rayner, J.-L. Imbach, M. Lee, J. A. Hartley, D.-K. Chang, J. W. Lown, *Nucleic Acids Res.* **1987**, *15*, 7027; see also further manuscripts of the senior author *J.-L. Imbach*, Montpellier, on this topic.
[24] F. Seela, H. Debelak, *Nucleic Acids Res.* **2000**, *28*, 3224.
[25] C. Boiziau, F. Debart, B. Rayner, J.-L. Imbach, J.-J. Toulme, *FEBS Lett*. **1995**, *361*, 41; F. Debart, G. Tosquellas, B. Rayner, J.-L. Imbach, *Bioorg. Med. Chem. Lett*. **1994**, *4*, 1041; M. Koga, A. Wilk, M. F. Moore, C. L. Scremin, L. Zhou, S. L. Beaucage, *J. Org. Chem*. **1995**, *60*, 1520.
[26] J. A. McDowell, D. H. Turner, *Biochemistry* **1996**, *35*, 14077.
[27] F. Seela, H. Driller, *Nucleic Acids Res.* **1989**, *17*, 901; T. Grein, S. Lampe, K. Mersmann, H. Rosemeyer, H. Thomas, F. Seela, *Bioorg. Med. Chem. Lett*. **1994**, *4*, 971; F. Seela, Y. He, C. Wei, *Tetrahedron* **1999**, 9481.
[28] F. Seela, I. Münster, U. Löchner, H. Rosemeyer, *Helv. Chim. Acta* **1998**, *81*, 1139.
[29] U. Sequin, *Experientia* **1973**, 1059.

Received February 23, 2001